ELECTROMAGNETIC FIELD DOSIMETRY
ELEKTROMAGNETNA DOZIMETRIJA

Peter Gajšek[1]

Prispelo: 1. 8. 2003 – Sprejeto: 1. 10. 2004

Review article
UDC 537.8

Abstract

In the last three decades, the use of devices that emit electromagnetic fields (EMF) has increased dramatically. The proliferation of EMF devices has been accompanied by concern about ensuring the safety of their use.
An important segment of the EMF research that looks after the biological effects of EMF is dosimetry which correlates external electric fields with those within tissues. Better methods are needed to properly measure, extrapolate or relate effects observed in animals to those expected to be found in people. The resulting data could lead to modification of existing safety standards or setting of new safety standards. Accurate dosimetry represents an essential element of the research in determining the biological effects of electromagnetic fields.
In the present paper, an overview over currently used experimental and numerical dosimetry methods in bioelectromagnetics research are given.

Key words: electromagnetic fields, dosimetry

Pregledni znanstveni članek
UDK 537.8

Izvleček

V zadnjih desetletjih se z izjemno hitrim razvojem novih tehnologij človekovo naravno in bivalno okolje temeljito spreminjata. Zaradi naraščanja števila naprav, ki so vir elektromagentnih sevanj (EMS), pa je med prebivalstvom vse bolj razširjen tudi strah pred morebitnimi negativnimi vplivi.
Pomemben element raziskav o vplivu EMS na organizme je dozimetrija, ki preučuje absorpcijo energije v biološki sistemu. Natančna dozimetrija pomaga raziskovalcem pri ponovitvah poizkusov. Računalniški modeli in numerične metode za oceno lokalizirane in telesne stopnje specifične absorpcije (SAR) se uporabljajo kot pripomoček pri načrtovanju številnih elektronskih naprav.
Pričujoči članek podaja pregled metod eksperimentalne in numerične dozimetrije, ki jih uporabljamo v raziskavah v bioelektromagnetiki.

Ključne besede: elektromagnetna sevanja, dozimetrija

Introduction

Electromagnetic energy is absorbed non-uniformly in biological tissues (1-3). Furthermore, a large number of factors such as a body's shape and position as well as its orientation in the field will produce non-uniform distributions (4-5). In short, there is no single answer to the question, "How much electromagnetic fields (EMF) will be absorbed in biological tissues?" Nevertheless, in order to make safe use of EMF emitting devices, a number of techniques for measuring EMF exposure have been devised. Unfortunately, all

[1]Doc. dr. Peter Gajšek, Institute of Non-Ionizing Radiation (INIS), Slovenčeva 95, 1000 Ljubljana
Correspondence to: e-mail: peter.gajsek@inis.si

have limitations. It is understandable then, why the development of mathematical dosimetry modeling techniques and sufficiently powerful computer hardware has resulted in the rapid adoption of dosimetry modeling as a principle tool in determining EMF exposure.
Computer-based dosimetry modeling provides great advantages by returning more information about an exposure than empirical techniques and with considerably less effort. But before this tool transitions into the hands of health safety officers and system designers, it must be verified under a wide variety of conditions using available analytical and empirical dosimetry techniques to verify its accuracy and limitations.
The state of empirical dosimetry has been reviewed (6) and is described in detail in the Radiofrequency Radiation Dosimetry Handbook (7). It is important to briefly review the techniques, as these will be the source of the empirical verification of any EMF dosimetry model.

Empirical Dosimetry

Baseline temperature measurements. Since absorbed EMF energy produces heat, measuring changes in temperature is the principal means of measuring EMF dose. To measure changes, a baseline temperature is required. One method is to allow the sample to equilibrate to the ambient temperature of the exposure chamber. An extended equilibration time is possible with stable samples; however, with biological specimens a long equilibration time is accompanied by changes in permittivity properties. An alternative procedure (8-9), which avoids this problem, is used with unstable samples such as biological tissues. Baseline temperature data is collected for a few minutes before and after the exposure. The average rate of temperature change during the non-exposure periods can be subtracted from the rate of change during exposure. The result is the rate of temperature change produced by the exposure. Using the specific heat for tissue of 0.84, a 1-degree C/minute temperature change is equal to a raw SAR of 58.6 W/kg (7). The raw SAR is then divided by the incident field intensity at the site of the measurement to convert to normalized SAR (W/kg/mW/cm^2). In this way, temperature changes due to other factors are isolated from changes due to EMF exposure. This allows the use of thermally unstable samples such as fresh carcasses.

Exposure parameters. In order to maximize sensitivity of samples to temperature changes resulting from EMF exposure and minimize the effects of other factors several considerations must be taken into account when selecting exposure parameters. First, power levels should be selected to produce as rapid a temperature rise as can be accurately detected, in other words, a relatively high incident power. Second, the exposure duration should be as brief as possible. The goal is to minimize the effects of thermal diffusion. Third, the temperature of the sample should be kept within the optimal sensitivity range of the thermometers being used. This may make it necessary to allow the sample to cool between separate exposures.

Measurement Techniques: Infrared Thermometry. A thermographic camera can be used to measure temperatures and consecutive SAR across the visible surface of an object (10). Since the camera is non-invasive it can be used in addition to other measurement techniques. A comparison of rendered three-dimensional SAR data and an infrared image can provide dramatic confirmation of finite-difference time-domain (FDTD) output (See Figure 1). Some samples (e.g., spheres and phantoms) can be constructed so that they can be quickly split after an exposure and scanned to visualize the temperatures over surface of the split. Care must be taken to ensure that the surfaces of the split had good electrical and thermal contact during the exposure.

Measurement Techniques: Calorimetry. Whole-body averaged SAR in phantoms and animal carcasses can be determined by twin-well calorimetry (11-14). Two identical samples are brought to temperature equilibrium. One is then exposed. Immediately after exposure, both are placed in the calorimeter wells. The calorimeter measures the heat diffusion for the exposed and unexposed samples, the difference is the amount of EMF energy absorbed by the exposed sample.

Measurement Techniques: Temperature Probes. Non-perturbing temperature probes are inserted into locations of interest. Baseline, exposure, and post-exposure temperatures are collected. Ideally, the temperature at the site of the probes will rise approximately one degree C during the exposure. These data are then analyzed to convert the temperature data to normalized SAR. Results for a phantom monkey at three frequencies are shown in Figure 2. FDTD predictions were used to guide the placement of the temperature probes.

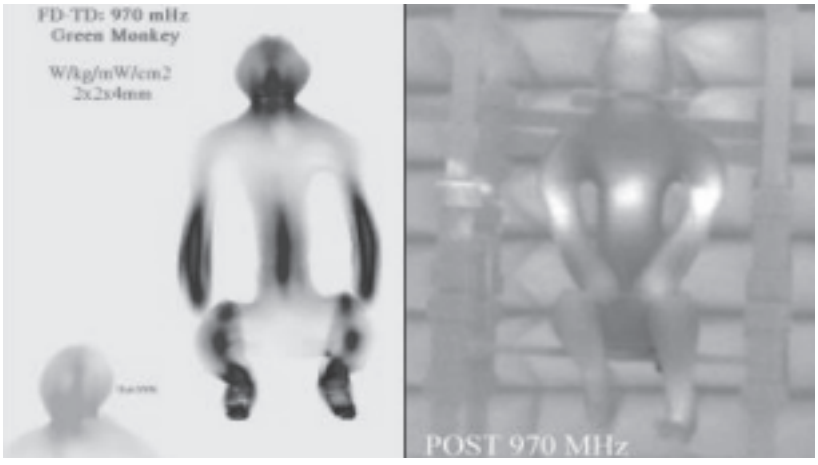

Figure 1. *The right panel shows infrared images of a monkey phantom exposed to 970 MHz. Higher temperatures are shown as white. On the left is a rendered image of the results of an FDTD analysis at the same frequency. Very low SARs are transparent, slightly higher SARs are purple, with the highest SARs shown as red. Both images show higher SARs in the arms, torso, ankles and neck. The very white area at the top of the phantom's head (right panel) is an artifact at the opening where the phantom was filled.*

Implantable E-field probes. This type of probes can be inserted into a sample in the same manner as the non-perturbing temperature probes just described. However, these probes measure the intensity of the E-field at the location of the probe. SAR can be directly calculated from the E-field (SAR = s÷E÷^{2}/rm ; where s=conductivity in siemens/meter, ÷E÷ is the electric-field strength in RMS volts/meter and rm is the mass density in kilograms/cubic meter). In addition, these measurements can be performed very quickly and at very low powers, so over heating of target is not an issue (6). The disadvantage of these probes is their lack of stability. Measurements are sensitive to many factors that would not alter a temperature-based system. As such these measurements must be performed with extreme care. Furthermore, the current generation of probes is quite large relative to the non-perturbing temperature probes; this increases the difficulty of using these probes with biological samples.

Dosimetry Samples

Cadavers. When the questions being addressed concern only SAR, a cadaver is preferable to a live animal, because a live animal's thermoregulatory system will confound temperature-based SAR measurements. However, the tissue will become dehydrated over time so it is best not to wait too long after the euthanization. If local SARs are to be measured, temperature probes will be implanted and temperatures recorded before, during and after exposures.

Spheres. The geometry of a sphere is artificial but very useful. Data collected from a homogeneous or multi-layered sphere are a useful test of the predictions of FDTD. The Mie theory (15) provides an important mathematically exact reference value for the sphere, which is easily modeled in both FDTD and the laboratory. First derived by Mie (15), this scattering solution is widely used in EMF and optics. Harrington (16) gives the exact solution in detail, and programs are available giving the exact near- and far-field results to which we can compare the FDTD results. Finally, because the MIE solution provides an exact value, sphere data can be used to measure error in the empirical values as well

Phantoms. Phantoms are constructed of an EMF-transparent fabric sewn into the desired shape and filled with a tissue-equivalent material. A variety of material recipes have been characterized for different simulated organs (muscle, fat, brain and bone) for a range of frequencies (14,17). Using the same mold, it is possible to place temperature probes in the same locations from session to session. Measuring SAR in phantoms is reproducible, convenient, and reduces the number of animals required. The whole-body SAR values with the

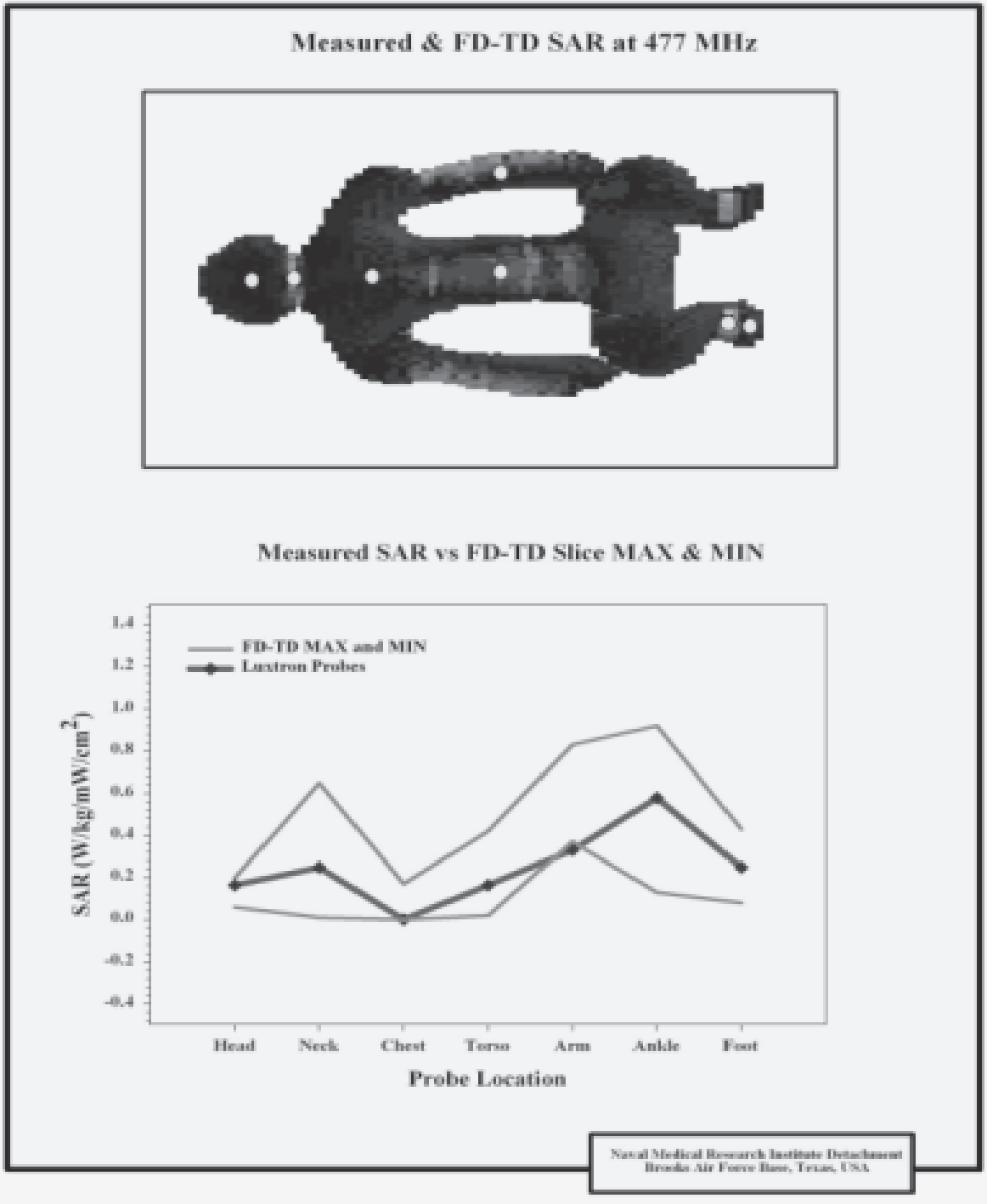

Figure 2. *A panel comparing FDTD results (rendered images and gray lines) to temperature probedata (red lines) at eight locations (yellow dots on images). The gray lines represent the range of SAR values in the area corresponding to the temperature probe location.*

rhesus monkey phantom are a good approximation of results observed with other methods. However, the localized SARs of the homogeneous phantom differ significantly from the structurally complex carcass and live animal. This differences must also be taken into account in bioeffects studies.

Numerical Dosimetry

The method most frequently used in EMF bioeffects dosimetry is the FDTD. As a finite difference algorithm, FDTD has the advantage of being able to analyze a wide variety of geometries. Unlike finite element method or method of moments, FDTD can be more efficiently applied to the very large problems such as a segmented version of the Visible Human male. These advantages have led to the rapid growth in the application and development of FDTD method.

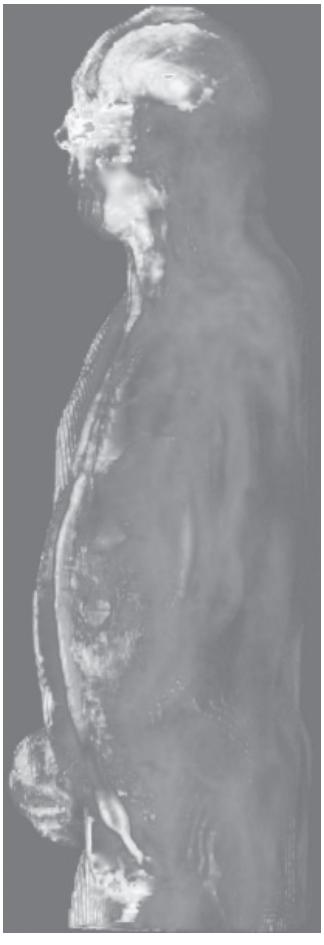

Figure 3. *Rendering of SAR results at 918 MHz using FDTD and 3 mm^3 man model.*

Finite-difference time-domain (FDTD). The FDTD method was originated by Yee (18) and later developed further by Taflove and colleagues (19-20); Holland (21), and Kunz and Lee (22). As more powerful computers became widely available, use of the FDTD method has increased exponentially (23-27 and http://www.fdtd.org). In addition, FDTD is widely used by manufacturers of cell phones to calculate head exposures during cell phone use.

The FDTD method is not limited to bioeffects research but it has been extensively used also to model antenna, waveguides, and military hardware. Unlike its main competitors, the method of moments (MOM) (28) and finite element method (FEM) (29), the FDTD method is scalable, i.e., the CPU time behaves linear in the problem size N. The MOM and FEM methods require matrix inversions (albeit sparse matrices in FEM) and thus scale as N^3. The MOM method is primarily useful for problems with conducting surfaces, but difficult to apply to permittivity problems of interest in bioelectromagnetics. Its practical limitation is to systems less than 10^6 cells. The FEM method, with its irregular cell structure, is difficult to parallelize efficiently. The FDTD method with its rectangular cell structure is easy to parallelize, and, in the case of the problem at hand, is compatible with the cellular data formats of the monkey and human anatomical models. The main disadvantages of FDTD are object resolution and absorbing boundary conditions (also in FEM), but sophisticated versions of the FDTD method have been developed to handle these problems (30). On the whole, we judge the FDTD approach to be the very useful in modeling the complex biological systems of interest.

FDTD Code. The FDTD program used at Brooks US Air-Force Base AFB is based on code originally developed by Kunz and Luebbers (31). It has been used to predict whole-body SAR and SAR distributions in spheres, monkey phantom, rhesus monkey, and human models. This FDTD program has been extensively used in the last few years to predict SAR in various models as part of ongoing bioeffects research. Continued development of the code by Luebbers and others has resulted in a commercial product X-FDTD (www.remcom.com).

We have made a number of modifications to the original code. We added more materials types to include all of Camellia Gabriel's types and some non-biological materials. The permittivity properties of each of the

tissue types are set according to data and fits published by Gabriel (32). Sample output for 918 MHz with the 3-mm version of the man model is show in Figure 3. The modified code reads the anatomical model files and outputs a 3-D normalized SAR file; mean, minimum, and maximum SARs for each tissue type; and each Z-plane slice. Finally, there is an extensive log file and all file names reflect run parameters. The code has been parallelized using the message-passing interface (MPI) library, which allows for larger and more complex data sets to be modeled. The advantage of using the MPI is that the code can run on parallel computer systems composed of networks of computers. These may be networked workstations, or massively parallel systems such as Linux-based Beowulf systems. These systems are easily constructed of inexpensive PC-hardware.

The visible human project: male data set

The human model is based on the photographic data from Visible Human Project created by the National Library of Medicine (www.nlm.nih.gov/research/visible/visible_human.html) and the University of Colorado Health Science Center (www.uchsc.edu/sm/chs). A computer-segmented set of the photographic images was created by National University of Singapore and Johns Hopkins University. We limited the number of tissue types based on their size in the body and availability of permittivity properties. Each of the 1878 slices in the XY plane was coded by hand using Adobe Photoshop ™ and a palette of colors that represented the 40 tissue types (See 33 for a complete description). It is the largest of the anatomical data sets we have created at 374 million voxels (1878 by 340 by 586). Each voxel is a cube 1 mm on a side. There are two improvements planned to enhance the usability of this data. First, the eyes will be opened. And second, the feet will be rotated and flattened slightly on the bottom to allow the model to make good contact with a ground plain or simulated shoe material. Modeling EMF exposures with this model will require approximately 18 GB of computer memory for FDTD. Smaller versions of this data set with resolutions of 2, 3, 5, 10 and 22 mm have been created and are suitable for some applications. These require considerably less memory but this savings come at a cost. The process would be as follows for creating a 3-mm anatomical model from a 1-mm model. Layers of air are added to one or more sides of the model volume to make the size of the model an even multiple of the 3 mm. The reduction would then take a cube of 3 by 3 by 3 one-millimeter voxels and based on the most common type in that cube create the single three-millimeter voxel. This process would be repeated for each 3 by 3 by 3 set of 1-mm voxels. As the voxel size increases small organs may be distorted or lost, some symmetries may be affected, organs will change mass slightly and the continuity of elongated structures may be disrupted. These reduced resolution models are created automatically.

International initiative - global EMF dosimetry project

One of the most useful documents in bioelectromagnetics is the Air Force Radiofrequency Radiation Dosimetry Handbook. Now in its 4th edition (7), the handbook describes, the principles and techniques for establishing EMF dose. It is a standard in radio frequency dosimetry. The International EMF Dosimetry Project was envisioned as the means of producing the next version of the dosimetry handbook. The International EMF Dosimetry Project was established as an international resource that provides state-of-the-science knowledge on EMF dosimetry. This project originated during the North Atlantic Treaty Organization (NATO) Advanced Research Workshop on Radio Frequency Radiation Dosimetry and Its Relationship to the Biological Effects of Electromagnetic Fields held at Gozd Martuljek, Slovenia, October, 1998.

The overall project goals of the International EMF Dosimetry Project are to promote the field of EMF dosimetry by creating internationally-accepted EMF Dosimetry Handbook and software that describe how EMF dosimetry measurements and calculations should be performed (www.emfdosimetry.org). By employing an open international forum, the Internet, the project should proceed rapidly, at low cost, and the results should be accepted internationally. This project could serve as the common ground for harmonizing EMF exposure standards that are currently unique to most countries.

Potential results of this project include: facilitation of international EMF research efforts and collaborations; assistance in EMF dosimetry predictions and measurements; development of an international research community that will identify EMF dosimetry research areas where further data are required; and rapid and easily accessible communication amongst researchers to avoid duplication of research efforts and maximize research costs. These results should permit more timely responses to the dosimetry requirements of the EMF community.

Conclusions

The empirical methods described in the previous sections have been the primary source of dosimetry data. However, these methods are labor intensive and may not be easily applicable to humans. In efforts to get more dosimetry information investigators have developed a number of techniques such as the use of phantoms. These techniques make the collection of dosimetry data more efficient. However, each also holds some compromises. In the case of the phantom mentioned above, it is homogeneous and only roughly shaped like the object it models. Other phantoms have been more realistic, but these are also more difficult to construct. It is not surprising that finite-difference models and high-resolution anatomical data sets would be readily adopted.

Despite of great progress over the last 30 years in RF dosimetry, there are some unsolved problems that still remain.. One of the foremost problems in theoretical dosimetry is incorporating the distribution of thermal energy due to blood flow (convective) or conductive cooling into numerical anatomical models. Further, it is important to continue performing experimental and theoretical research to improve the accuracy of permittivity data across the electromagnetic spectrum. Recent reports indicate that live bone may have dielectric parameters that are closer to those of muscle, i.e. higher dielectric value and conductivity, than assumed previously. New data would also suggest that an overestimation has occurred in brain SAR data in past dosimetric studies that used tissue-equivalent or computer models. Special attention should be paid also to permittivity values of different biological tissues at lower frequencies where the differences in reported data are more than one order of magnitude. In parallel, extended studies on parametric dependence of SAR on permittivity values at lower frequencies would also be needed.

Overall, we have determined that the two approaches (theoretical and empirical) to RF dosimetry are complementary, and as both have certain advantages and limitations, these should be considered in selecting one or the other or both approaches to solve a certain dosimetric problem. It is only with continued dosimetry research that the development of electromagnetic technology can be fostered safely for the benefit of mankind while avoiding unreasonable restrictions.

References

1. D'Andrea JA; Gandhi OP; Lords JL: Behavioral and thermal effects of microwave radiation at resonant and nonresonant wavelengths. Radio Sci. 12(6S): 251-256; 1977.
2. D'Andrea, JA; Emmerson, RY; Bailey, CM; Olsen, RG; Gandhi OP Microwave radiation absorption in the rat: Frequency-dependent SAR distribution in body and tail. Bioelectromagnetics 6: 199-206; 1985.
3. Gandhi OP.; Hagmann MJ; D'Andrea JA: Partbody and multibody effects on absorption of radio frequency electromagnetic energy by animals and by models of man. Radio Sci. 14(6S): 15-22, 1979.
4. Durney CH, Johnson CC; Barber PW; Massoudi H; Iskander MF.; Lords, J.; Ryser DK; Allen SJ; Mitchell JC: Radiofrequency radiation dosimetry handbook. SAM-TR-78-22, Brooks Air Force Base, San Antonio, TX, 1978.
5. Gandhi OP: Polarization and frequency effects on whole animal energy absorption of RF energy. Proc. IEEE 62: 1171-1175, 1974.
6. Chou CK, Bassen H, Osepchuk J, Balzano Q, Petersen R, Meltz M, Cleveland R, Lin JC, Heynick L Radio frequency electromagnetic exposure: tutorial review on experimental dosimetry. Bioelectromagnetics. 1996;17(3):195-208.
7. Durney CH; Massoudi H; Iskander MF: Radiofrequency radiation dosimetry handbook. USAFSAM-TR-85-73, Brooks Air Force Base, TX, 1986.
8. Gambrill CS, DeAngelis ML, Lu ST: Error analysis of a thermometric microwave-dosimetry procedure. In: Blank M, editor. Electricity and magnetism in biology and medicine, San Franscisco: San Francisco Proess. 593-595.
9. Lu ST, DeAngelis ML, Gambrill CS. Ocular microwave thermometric dosimetry and thermometry in the rabbit. In: Blank M, editor. Electricity and magnetism in biology and medicine. San Francisco: San Francisco Press, Inc. 675-678; 1993.
10. Mason PM, IR mapping for greater radiation safety. Electronics Tech Briefs, 11-13 April 1999.
11. Phillips RD, Hunt EL, King NW, Field measurements of absorbed dose and biologic dosimetry of microwaves. Ann NY Acad Sci 247:499-509, 1975.
12. Blackman CF, Black JA, Measurement of microwave radiation absorbed by biological systems. 2. Analysis by Dewar-flask calorimetry. Radio Science 12(65):9-14, 1977.
13. Allen SJ, Hunt WD, Calorimetric measurements of microwave energy absorption by mice after simultaneous exposure of 18 animals. Radio Science 14(65):1-4, 1979.
14. Chou CK, Chen GW, Guy AW, Luk KH, Formulas for preparing phantom muscle tissue at various radiofrequencies. Bioelectromagnetics 5:435-441,1984.
15. Mie G: Contributions to the optics of diffusing media. Ann Physik, 25,1908.
16. Harrington RF, "Time Harmonic Electromagnetic Fields", McGraw-Hill Book Company, New York, 1961, pp. 264-316.
17. Guy AW, Analyses of electromagnetic fields induced in biological tissues by thermographic studies on equivalent phantom models. IEEE Trans Microwave Theor Tech 19:205-214, 1971.
18. Yee KS, Numerical solution of initial boundary value problems involving Maxwell's equations in isotropic media. IEEE Transactions on Antennas and Propagation, Vol. 14, p. 302, 1966.
19. Taflove A and Brodwin ME, Computation of the electromagnetic fields and induced temperatures within a model of the microwave irradiated human eye, IEEE Transactions on Microwave Theory and Techniques, MTT-23, 888, 1975.

20. Taflove A and Umashankar KR, The finite-difference time-domain method for numerical modeling of electromagnetic wave interactions with arbitrary structures, Chapter 8 in Progress in Electromagnetics Research, PIER 2, Michael A. Morgan, Editor, Elsevier Science Publishing Company, New York, 1990.
21. Holland R: THREDE: A fore-field EMP coupling and scattering code, IEEE Transactions on Nuclear Science, Vol. 24, p. 2416, 1977.
22. Kunz KS, and Lee KM: A three-dimensional finite-difference solution of the external response of an aircraft to a complex transient EM environment, 1. The method and it's implementation. IEEE Transactions on Electromagnetic Compatibility, Vol. 20, p. 328, 1978.
23. Shlager KL and Schneider JB, A Selective Survey of the Finite-Difference Time-Domain Literature. *IEEE Antennas and Propagation Magazine*, 37:4, pp. 39-56, 1995.
24. Gandhi OP: Some Numerical Methods for Dosimetry: ELF to microwave frequencies. Radio Science, Vol. 29, November, 1994.
25. Stuchly MA, Gandhi OP Inter-laboratory comparison of numerical dosimetry for human exposure to 60 Hz electric and magnetic fields. *Bioelectromagnetics* 2000 Apr; 21(3):167-74
26. Dimbylow PJ, FDTD calculations of the whole-body averaged SAR in an anatomically realistic voxel model of the human body from 1 MHz to 1 GHz. Physics in Medicine and Biology, Vol 42, pp. 479-490, 1997.
27. Gajšek P, Ziriax JM, Hurt WD, Walters TJ, and Mason PA: Predicted SAR in Sprague-Dawley rat as a function of permittivity values, Bioelectromagnetics 24, 1-17, 2001.
28. Harrington RF, "Field Computation by Moments Method", The Macmillan Company, New York, 1968.
29. MacNeal BE, editor, "MSC/EMAS Modeling Guide", The MacNeal-Schwendler Corporation, 1991.
30. Taflove A "Computational Electrodynamics – The Finite-Difference-Time_Domain Method", Artech House, Boston, 1995.
31. Kunz KS and Luebbers RJ: "The Finite Difference Time Doman Method for Electromagnetics", CRC Press, Inc., Boca Raton, FL, 1993.
32. Gabriel C: Compilation of the Dielectric Properties of Body Tissue at RF and Microwave Frequencies, Brooks AFB, TX: Armstrong Laboratory Report, AL/OE-TR-1996-0037, 1996 (www.starview.org).
33. Mason PM, Walters TJ, Fanton JW, Erwin DN, Gao JH, Roby JW, Lott KA, Lott LE, Blystone RV. Database created from magnetic resonance images of a Sprague-Dawley rat, rhesus monkey, and pigmy goat. FASEB J., 9:434-440, 1995.